PLANKTON RESPONSE TO WEAKENING OF THE IBERIAN COASTAL UPWELLING

Fiz F. Pérez*, Xosé. A. Padín*, Yolanda Pazos†, Miguel Gilcoto*, Manuel Cabanas‡ , Paula C. Pardo*, Mª Dolores Doval† and Luis Farina-Busto§,

*Instituto de Investigaciones Marinas, CSIC, Eduardo Cabello 6, E-36208 Vigo, Spain

†Instituto Tecnolóxico para o Control do Medio Mariño de Galicia. Peirao de Vilaxoan, E-36611 Vilagarcia de Arousa. Spain

‡Centro Oceanográfico de Vigo, Instituto Español de Oceanografía, Cabo Estay, 36200-Vigo, Spain

§Facultade de Ciencias do Mar, Universidade de Vigo , Campus de Lagoas-Marcosende, E-36310 Vigo, Spain

Corresponding author Fiz F. Pérez

e-mail: fiz.perez@iim.csic.es

Fax: (+34) 986 292 762

Phone: (+34) 986 231 930 Ext. 360

Keywords: coastal upwelling, climate change, plankton succession, coastal ecosystem

Version: November 4th, 2009

Submitted to: Global Change Biology

Running Title: Upwelling weakening and plankton response.

A Candidate Cover Image has been proposed with the caption:

Long-term decrease of upwelling (curve with experimental points) related to climate evolution in the Northeast Atlantic (under the curve) induces predominance of Dinoflagellates (upper right corner) and Pseudonitzschia spp over Diatoms (lower left corner) in coastal areas, reducing the productivity of exploitable species (mussel culture in the Galician Rias, over the curve).

Abstract. Coastal upwelling regions, which are affected by equatorward-wind variability, are amongst the most productive areas of the oceans. It has been suggested that global warming will lead to a general strengthening of coastal upwelling, with important ecological implications and an impact on fisheries. However, in the case of the Iberian upwelling, the long-term analysis of climatological variables described here reveals a weakening in coastal upwelling. This is linked to a decrease of zonal sea level pressure gradient, and correlated with an observed increase of sea surface temperature and North Atlantic Oscillation. Weakening of coastal upwelling has led to quantifiable modifications of the ecosystem. In outer shelf waters a drop in new production over the last 40 years is likely related to the reduction of sardine landings at local harbors. On the other hand, in inner shelf and Ria waters, the observed weakening of upwelling has slowed down the residual circulation that introduces nutrients to the euphotic layer, and has increased the stability of the water column. The drop in nutrient levels has been compensated by an increase of organic matter remineralization. The phytoplankton community has responded to those environmental trends with an increase in the percentage of dinoflagellates and *Pseudonitzschia spp* and a reduction in total diatoms. The former favors the proliferation of Harmful Algal Blooms and reduces the permitted harvesting period for the mussel aquaculture industry. The demise of the sardine fishery and the potential threat to the mussel culture could have serious socio-economic consequences for the region.

Introduction

Coastal upwelling occurs along the eastern ocean margins when along-shore equatorward winds drive the surface layer offshore, inducing the rise of deep, cool, and nutrient-rich waters into the coastal photic layer. These nutrient pulses fuel the high phytoplankton production that supports rich coastal marine ecosystems and productive fisheries (Pauly & Christensen 1995). The duration of the seasonal cycle of upwelling-favorable winds (as well as their strength) varies along the coast (Wooster et al. 1976), affecting the development of 'blooms' of different phytoplankton species (Anderson, 1997).

Understanding of climatic modulations of the intensity of coastal upwelling has become increasingly important because of the likelihood of dramatic ecosystem and socioeconomic impacts (Bakun & Weeks, 2004, Barth *et al.* 2007). It has been argued that the expected and observed sea surface temperature (SST) increase due to global warming might induce the intensification of coastal upwelling (Bakun 1990). In the California Current System, a positive trend in upwelling-favorable winds along Southern California coexists with an increase of SST driven by surface heat fluxes; however the net warming trend is accompanied by an increased stratification and a deepening of the thermocline that reduces the efficiency of upwelling (Di Lorenzo *et al.* 2004). The IPCC Reports argue that an enhancement of the planetary capacity to retain energy received from the sun ("global warming") will not always lead to local temperature increases. In the Atlantic Ocean, analysis of the North Atlantic Oscillation (NAO) has shown that large-scale atmospheric modes may lead simultaneously to local effects of opposite signs. The first mode of NAO shows a tri-polar distribution of the SST anomaly distribution in the North Atlantic (Visbeck *et al.* 2001); the study area (Fig. 1) lies in an ocean margin region equally distant from these three centres.

Long-term variability in upwelling systems is coupled to changes in the ecosystem productivity and may influence the frequency of harmful algal blooms (HABs; GEOHAB, 2005). In the large coastal upwelling systems of SW Africa, Peru–Chile, California–Oregon and Somalia, Gregg *et al.* (2005) relate the significant increase of chlorophyll *a* measured from space to a positive trend of the upwelling-favorable winds along those coasts. A long-term increase in northerly wind component over the eastern North Atlantic between 1950 and 1980 was associated both with a decline of phytoplankton and zooplankton biomass in sea-areas around the British Isles, and with an increase in upwelling intensity along the Iberian west coast (Dickson *et al.* 1988). From a long temperature and phytoplankton data set, Wiltshire & Manly (2004) found a first indication of a warming-related shift in phytoplankton succession in the North Sea system. NAO variability has also been linked to phytoplankton dynamics in coastal systems by some authors (Belgrano *et al.* 1999, Irigoyen *et al.* 2000, Wasmund & Uhlig 2003), while others focused on the relation between NAO and open sea plankton (Jossi et al. 2003, on the Continuous Plankton Recorder Survey).

In spite of the described effects of climate variability on the oceanic ecosystems, long term observations showing biogeochemical trends due to changes in physical forcing are quite scarce. The socioeconomic importance of the Iberian Upwelling has stimulated the collection of an interdisciplinary database of high-frequency long-term observations. On the basis of the analysis of the climatological data we will show an unexpected weakening of the Iberian Upwelling. This clearly affects the chemical and biological ocean environment, producing different responses of the ecosystem in the open sea and in the inner shelf. By considering underlying processes, we attempt to clarify how open sea and inner shelf ecosystems are responding and infer, qualitatively, the economic consequence of such ecological changes.

Methods

In this section we give details on the methods used for data analysis: upwelling index (Iw), satellite chlorophyll *a*, New Production (NP), Net Ecosystem Production (NEP) and hydrographic and phytoplankton monitoring in Ría de Arousa. Upwelling index series in the Iberian upwelling region is being calculated four times a day since 1966 by the IEO Vigo (Cabanas & Alvarez 2005). In order to assess the long-term variability of the biological activity in the outer shelf we calculated yearly averages of NP from Iw from 1966 to 2006. In Ría de Arousa, 15 years long time series of hydrographic and phytoplankton data from three inner-shelf stations of the ecosystem monitoring network maintained by the local Government (Pazos & Maneiro 1994) are presented and their trends analyzed. NEP is then calculated from Iw in Ría de Arousa to complete the picture.

Description of the study area. The Iberian coast is located in the northern limit of the North Atlantic Upwelling System (Fig. 1). It is one of the world's major upwelling areas; it is a highly productive locus of intensive fisheries and constitutes the Canaries–Iberian Large Marine Ecosystem (Longhurst 1996). A weak southward Portugal Current offshore of Iberia and the Azores Current contribute to the Canary Current. Underneath, a poleward undercurrent flows as a slope current from the African coast as far north as Bay of Biscay (Pingree & Le Cann 1990). These oceanographic features are dominantly modulated by the seasonal cycle of the wind direction. This follows the position and strength of the Azores High and the predominance of northeast winds from May to October is the main cause of upwelling (Wooster *et al.* 1976). A detailed review of the main oceanography and biological characteristics are given by Aristegui et al. (2006).

Upwelling index computations. The northerly component of shelf wind stress (τ_y) causes upwelling-favorable offshore Ekman transport along the western Iberian margin, and southerly winds result in the opposite effect, i.e. downwelling and onshore transport.

Ekman transport or upwelling index (Iw m^3 s^{-1} km^{-1}) can be estimated by Bakun's method (Bakun 1973):

$$I_w = -\frac{\tau_y}{\rho_{sw} f} = -\frac{\rho_{air} C_D |V| V_y}{\rho_{sw} f} \qquad (1)$$

where ρ_{air} is the density of air (1.22 kg·m^{-3} at 15ºC), C_D is an empirical dimensionless drag coefficient (1.4 10^{-3}), f is the Coriolis parameter (9.946·10^{-5} s^{-1} at 43º N), ρ_{SW} is the density of seawater (~1025 kg m^{-3}), and |V|, V_y are respectively the average daily strength and northerly component of the wind. Positive (negative) values of Iw corresponds to upwelling (downwelling) in the Iberia Upwelling System.

Because the upwelling index does not reflect the full complexity of the phenomenon it quantifies, it is advisable to study its evolution with various different data sources, thus two upwelling indices have been calculated for this work. SLP Iw denotes an upwelling index calculated using geostrophic winds within a 2º x 2º cell centered at 43ºN 11ºW (Fig. 1), representative of the working area. Geostrophic winds were calculated from atmospheric sea level pressure (SLP) charts (four maps per day) provided by the *Instituto Nacional de Meteorología* (Cabanas & Alvarez 2005). NCEP Iw is calculated with equation 1 using winds (four per day at 42.853 ºN and 9.37 ºW) from the reanalysis carried out by Kalnay *et al.* (1996).

Chlorophyll a data from space. Remotely sensed Chlorophyll *a* products are freely provided by the Sea-viewing Wide Field-of-view Sensor (SeaWiFS) and Moderate Resolution Imaging Spectroradiometer (MODIS) projects and GeoEye at http://oceancolor.gsfc.nasa.gov, covering the period from 1997 to 2007. The performance of the SeaWiFS sensor has demonstrated remarkable consistency for most of the mission. However, there were some quality problems at the end of the latter period, already beyond the design lifetime of the instrument (http://oceancolor.gsfc.nasa.gov/REPROCESSING/SeaWiFS/R5.2/cal_drift.html). From 2003 remotely sensed chlorophyll *a* is also provided by the MODIS project. In order to complete the chlorophyll *a* data base with recent observations we took the MODIS level-3 products and kept 2 years (2003-2005) of overlap with SeaWiFS level-3 data products.

New Production in the outer shelf. "New Production" is the fraction of gross production maintained by external nutrients (Eppley & Peterson 1979). In upwelling regions those are the nutrients transported by the upwelled water. This is the basis of the trophic chain on the outer shelf. Álvarez-Salgado *et al.* (2002) developed an algorithm for calculating NP on the basis of upwelling index, using data from a total of 128 casts in the area between 42ºN and 43ºN and between 11ºW and to the East the position of the 1000 m depth isobath, from 14 hydrographic cruises conducted in the Iberian shelf from 1977 to 1998. The fortnight-average of Iw (Iw(f)) allows the estimation of the fortnight-average NP (in $\mathrm{mg\,C\,m^{-2}\,day^{-1}}$), through:

$$NP(\pm 197) = [(1.1 \pm 0.1) + (5 \pm 0.1) \cdot 10^{-4} \cdot I_W(f)] \cdot I_W(f) + (0.15 \pm 0.04) \cdot I_W(f-1) \qquad (2)$$

There is a marked influence of the average upwelling rate during the previous fortnight (*f*-1). The evaluated NP has been tested against satellite-derived net microbial community production during 1998-1999 (Álvarez-Salgado *et al.* 2002).

Ecosystem monitoring network in Ría de Arousa. The Rías Baixas are four large embayments (2.7 to 4.8 km^3) open to the oceanic influence from the adjacent shelf. *Ría de Arousa* is the most extensive of the four (4.8 km^3). It is well connected to the shelf by a deep and wide mouth receiving the strong impact of upwelling. It has a two-layer circulation, strongly affected by wind over the open shelf. With northerly winds, the induced upwelling accelerates the vertical and horizontal positive estuarine circulation;

instead, southerly winds slow down the estuarine circulation or even produce a reverse estuarine circulation (Rosón et al. 1997).

The edible mussel aquaculture production in Ría de Arousa amounts to a quarter of a million tons per year from 2396 rafts, being one of the world's biggest. A local government agency (*Instituto Tecnolóxico para o Control do Medio Mariño*, http://www.intecmar.org/) maintains since 1992 an extensive network of 38 oceanographic stations for monitoring HAB events and provides weekly hydrographic and phytoplankton data (Pazos & Maneiro 1994). In this work data from three stations in the outer part of Ría de Arousa are used to study the hydrographical and phytoplankton variables. These coastal stations are directly subjected to the outer shelf dynamics; stations located in the inner Ría are much more under the influence of land-coastal processes, such as run-off, and for this reason are not considered here. Hydrographic vertical profiles with a Sea-Bird 25 CTD are carried out, measuring salinity and temperature in the water column. Here only the mean averages of the upper 15 meters, where nutrients and phytoplankton species composition are monitored, are described. The water column is sampled in three depth intervals: from the surface to 5 meters, from 5 to 10 meters and from 10 to 15 meters, by means of a hose following the Lindhal technique (Sutherland *et al*. 1987). From these samples, the analysis of pigment composition, nutrient concentrations and the counting of phytoplankton cells are conducted. Chlorophyll *a* is measured spectrofluorometrically (Zapata *et al*. 1994). Nutrient concentrations are determined according to Hansen & Grasshoff (1983) using standard segmented flow analysis with TRACCS 800-2000 and Quattro systems. Lugol's fixed samples are taken for phytoplankton abundance using the sedimentation technique in Uthermöhl chambers and examining them under an inverted microscope.

The variables studied here have a strongly seasonal component, due to their dependence on annual physical environmental variables (light, heat absorption, winds etc.). We thus follow the standard procedure of separating the seasonal cycle (fitted to six harmonics: 1, 1/2, 1/3, 1/4, 1/5 and 1/6 years) before the analysis of long-term trends. To determine the linear decadal trend (*m*) of nutrient concentrations and phytoplankton descriptors, each variable was fitted to an expression of the form

$$Var = a_0 + m \cdot (t/3652.5) + \sum_{i=1}^{6} b_i \sin(2\Pi i \cdot (t - f_i)/365.25) \qquad (3)$$

where *t* is time in days and a_o, b_i *y* f_i are the fitting parameters.

*Net Ecosystem Production in the inner shelf***.** Using total inorganic carbon, nutrient and oxygen data and a two-layered kinematic box model constrained by non-steady salt and thermal budgets, Pérez *et al.* (2000) estimated the Net Ecosystem Production (NEP) from spring to autumn of 1989 in Ría de Arousa. Afterwards, NEP was empirically correlated with several physical variables (upwelling, stability and surface heat flux) seeking the linear combination of Iw, Brunt-Väisälä frequency (BV) and irradiance (F) which better explained the time evolution of NEP (in mmol O_2 m^{-2} day^{-1}). The best fit ($r^2 = 0.70$) was obtained with the equation:

$$\begin{aligned} NEP = {} & [(70 \pm 16) \cdot 10^{-3} I_W(d_{0-3}) - (35 \pm 14) \cdot 10^{-3} \cdot I_W(d_{4-10})] + \\ & (0.38 \pm 0.06) \cdot (F(d_{0-3}) + F(d_{4-6})) - (198 \pm 37) BV(d_{0-6}) \qquad (4) \end{aligned}$$

where *F* is in cal cm^{-2} day^{-1}, *BV* is in s^{-1}, *d* stands for days and the sub-index stands for the number of days backwards used to do the average, i.e. $Iw(d_{4-10})$ is the average *Iw* from 10 to 4 days before the date for which NEP is computed. The above equation permits to estimate the annual averaged NEP of Ría de Arousa using daily Iw assuming a seasonal cycle of Brunt-Väisälä and irradiance.

Results and discussion

Long-term upwelling variability. Figure 2 shows the two upwelling indices calculated here, for the years between 1966 and 2006, reduced to their mean annual averages. The linear trends, which are qualitatively consistent, are also shown. NCEP Iw has a significant decrease of -44 ± 14 $m^3 s^{-1} km^{-1}$ $decade^{-1}$ ($P = 0.0015$). SLP Iw has a steeper decrease of -47 ± 16 m^3 s^{-1} km^{-1} $decade^{-1}$ ($P = 0.002$). Monthly SST from NCEP is also shown in Figure 2. A clear warming from 1972 to 2006 is apparent, with a mean rate of 0.29 ± 0.03 ºC $decade^{-1}$ ($P < 10^{-5}$). Both upwelling indices show a significant negative correlation with NCEP SST ($P = 7 \cdot 10^{-4}$ for SLP Iw and $P = 0.015$ for NCEP Iw).

To illustrate further the long-term variation of the upwelling indices and their relation to other climatological trends we consider in more detail two strongly contrasting periods, one at the beginning and another one at the end of the four decades studied. Figure 1 shows contours of average SLP for June, July and August of 1973-74-75 (red) and 2001-02-03 (black) superimposed on SST differences between these periods. The focus is on summer months because these are the most relevant ones for upwelling. Only slight changes of SLP cross-shore gradient along NW Africa coast are apparent; on the other hand, significant decreases in the zonal gradient at latitudes over 40ºN are observed. There, isobars open up and separate with a reduction of the zonal gradient of SLP over these thirty years, at 43ºN, of about 30% (see the pink segment in Fig. 1, crossing the study area). Changes in the isobars pattern in the Bay of Biscay between both periods are striking, making geostrophic winds shift from northerlies during the '70s to westerlies after 2000.

During these three decades, two regional trends in the changes of the summer SST can be identified. A slight cooling can be observed around Cape Ghir, where colder surface waters appear, in agreement with the results from sediment cores (McGregor et al. 2007), and north of 45ºN. In all other North East Atlantic areas, the mean summer SST increases by about 1ºC during these three decades. Shelf and oceanic water off the Iberian Peninsula show a significant warming as well. All these results agree with previous basin-scale and long-term studies of evolution of SLP and SST in the context of the NAO signal (Visbeck et al. 2001). Monthly NAO and SLP Iw show a positive correlation of r = 0.2 (P = 0.0002, n = 478, slope 0.093±0.021 $m^2 s^{-1}$). Using the recently described summer NAO for June, July and August (SNAO) index (Folland *et al*. 2009) a clear relation is found: the correlation between the summer mean of SNAO and SLP Iw improves significantly the linear fit (r = 0.52, P = 0.006, slope 0.27±0.07 $m^2 s^{-1}$). On the other hand, summer mean SNAO and the Iw in cape Ghir (NW Africa) show an inverse correlation (r = -0.3, P = 0.01, slope = –0.121±0.048 $m^2 s^{-1}$). This opposite correlation agrees with the known correlation pattern between wind curl (cyclonic pattern) and NAO, negative in the study area and positive around cape Ghir (Marshall et al. 2001). During the positive phase of NAO (1973-75) an increase of anticyclonic activity off NW Iberia favors upwelling, while during a negative phase (2002-04) upwelling is weakened, in agreement with the change of SLP pattern (Fig. 1).

Ecological outer shelf trends. Several authors have noted that changes in the upwelling intensity related to global warming would produce significant socioeconomic impacts (Pauly & Christensen 1995, Bakun & Weeks 2004, Barth *et al.* 2007). We can show a first quantitative measure of this impact by means of the correlation between NP and sardine landings over the four decades from 1965 to 2006.

The sardine (*Sardine pilchardus*) is a small plankton-eating pelagic fish with a northward migration pattern around the Iberian Peninsula. Its early growth depends critically on the nutrients brought about by upwelling and the corresponding NP. During summer and autumn the bulk of the recruits at age 0 are found off the northern coast of Portugal, just south of our sampling area. There is a northward age gradient pattern from Western Iberia, where most of the fish are young, to the Cantabrian Sea where the bulk of the population belongs to older age groups. This suggests a northward feeding migration (Carrera & Porteiro 2003). The landings of sardine from Bay of Biscay (Division VIIIc of ICES, ICES 2007; http://www.ices.dk/committe/acom/comwork/report/2007/oct/sar-soth.pdf) show a maximum during the early '70s and a progressive decrease since (Fig. 3). Yearly averaged NP in the area of early growth computed from the SLP Iw (Fig. 3) has a significant time-correlation with annual landings of sardine in the Bay of Biscay ($r = 0.69$, $P < 0.00001$, $n = 36$). This suggests that the strong decline in sardine stocks is related to the decline of coastal upwelling off NW Iberian Peninsula. Although other processes, like warming and overfishing have been invoked to explain the decrease of the sardine stock (Carrera & Porteiro 2003), the high percentage of explained variability in the sardine landings is new quantitative evidence to support the argument that the weakening of the coastal upwelling intensity is causing an important impact in pelagic life (Pauly & Christensen 1995).

Inner shelf upwelling trends. The consequences of the weakening of coastal upwelling on the biological parameters described above cannot be directly extrapolated to the Rías located in this coastal upwelling region. We show in Fig. 4 the spatial average between the three external stations in the Ría de Arousa for seven parameters (SST, chlorophyll *a*, diatom, dinoflagellate and *Pseudonitschia spp.* abundances, nitrite, ammonium and phosphate) measured at the monitoring network between 0 and 15 meter of depth. Although the SST at the external end of Ría de Arousa shows (Fig. 4) a warming of

0.27±0.1 ºC decade^{-1} (P = 0.005) that follows the long-term pattern of ocean waters (Fig. 2), the chlorophyll *a* concentrations have been increasing (Fig. 4) at interannual scales with a rate of 1.2±0.4) mg m^{-3}decade^{-1} (P = 0.005) in opposition to the decreasing trend on the outer shelf. Between 1997 and 2006 (Fig. 4) surface chlorophyll *a* from SeaWiFS/MODIS sensors in the outer Galician and Northern Portugal shelf shows a decreasing trend of –0.2±0.08 mg m^{-3} decade^{-1} (P = 0.04) in agreement with the observed oceanic trends found in stratified conditions associated with the SST warming (Behrenfeld *et al.* 2006, Gregg *et al.* 2005).

In upwelling systems it is well known (Bakun & Weeks 2004) that a recirculation of coastal water creates a near-bottom layer along the shelf which accumulates the mineralized organic matter generated in the photic layer of the inner shelf by the upwelled nutrients. The nutrient concentrations may increase by more than 100% (Fraga 1981). This layer is recurrent in all upwelling systems; it has been found along the shelf of the Iberian Peninsula (Alvarez-Salgado *et al*. 1997), and it is more evident toward the end of upwelling seasons when the intensity of upwelling decreases while the stratification in the water column increases. Thus, the upwelled water that fertilizes the inner shelf bears more nutrients than expected on the basis of the intensity of upwelling, particularly when it is weak (Fraga 1981). To verify that this might be the mechanism that reverses the chlorophyll *a* trend between outer and inner shelf waters, we study the monthly averaged nutrients in the upper 15 meters in the external end of Ría de Arousa (Fig. 4). Nitrate concentrations show no significant trend (not shown) while nitrite, ammonium and phosphate concentrations follow positive significant trends of 0.11±0.04 (P = 0.006), 0.20±0.09 (P = 0.04) and 0.11±0.02 ($P = 2\cdot10^{-8}$) respectively, all in µmol L^{-1} decade^{-1} (Fig. 4). This leads to a negative trend in the total inorganic nitrogen/phosphate ratio of -1.8±0.9 decade^{-1} (P = 0.05). These trends fit very well with a pattern of increase of remineralized nutrients from fresh organic matter: nitrogen originated from recently decomposed organic tissues has a higher fraction of nitrite and ammonium with respect to nitrate than in upwelled waters. This mechanism allows the Ría to support a high biological activity despite a persistent weakening of upwelling intensity. In fact the NEP in the Ría of Arousa obtained from an empirical model (see methods) yields a barely (statistically non significant) negative trend during the last 15 years, an order of magnitude lower than that corresponding to the outer shelf.

Inner shelf plankton response. The change of coastal upwelling intensity, the warming and nutrient-ratios trends can produce alterations in the phytoplankton community. Superimposed on the annual cycle, the succession of phytoplankton species in Ría de Arousa from diatoms to dinoflagellates is controlled by upwelling and stability (Pazos *et al.* 1995). The abundance of total diatoms shows a decreasing trend of -0.14 ± 0.04 log (cells L^{-1}) decade^{-1} ($P = 0.001$) while the percentage of total dinoflagellate is increasing at a steady rate of 0.11 ± 0.06 log(%) decade^{-1} ($P = 0.05$) as predicted by Margalef's Mandala (Margalef *et al.*1979, Smayda & Reynolds 2001). Despite the decrease of total diatom cells, the phytoplankton assemblage *Pseudonitschia spp.*, which includes shellfish-poisoning amnesic-toxin producers, shows a very significant ($P = 5.10^{-5}$) increase of 0.48 ± 0.12 log (cells L^{-1}) decade^{-1}. There is also a negative trend in the total number of cells -0.14 ± 0.03 log (cells L^{-1}) decade^{-1} ($P < 0.00001$) which is opposed to the positive trend in chlorophyll *a* concentrations. It appears that the less turbulent environment induced by the sea surface warming and the weakening of the coastal upwelling is favoring taxa of larger cell size as found by Smayda & Reynolds (2001). Indeed, similar trends in cell size were found in association with climate-warming scenarios coupled with water-column stratification (Johns *et al.* 2003).

Some authors have suggested that HABs are increasing globally due to anthropogenic influences (Smayda *et al.* 2004) while others have stressed that climate variability (apart from increased monitoring and awareness) may be as equal contributor (Anderson, 1997, Sellner *et al.* 2003). From the relationship between Iw and estuarine circulation given by Rosón *et al.* (1997), an evaluation of the impact of coastal upwelling on residence times of upwelled water in Ría de Arousa shows a decadal slowdown of the flushing times of 1.1±0.2 days ($P = 2\cdot10^{-5}$) due to weakening of upwelling. This trend is even larger in summer (1.7±0.5 days per decade, $P = 0.001$) representing a reduction rate of the renewal time nearly 10% per decade. This decrease could exacerbate the impact of the terrestrial anthropogenic fertilization since it would drive the coastal ecosystem towards eutrophication.

These changing patterns that relate phytoplankton dominance and climate variability are relevant to understanding the evolution and occurrence of HABs. If these climatic changes persist, they may lead to the emergence of a new successional regime in phytoplankton and to the formation of earlier and more frequent dinoflagellate blooms (Alvarez-Salgado *et al.* 2008).

Summary

We observed a weakening of the Iberian upwelling coincident with an increase of sea surface temperature (SST). This weakening appears to be related to the reduction of the SLP zonal gradient and might be coupled with the summer NAO. We also found a clear relationship between North Iberian sardine landings and upwelling strength, understandable in terms of the influence of the West Iberian coastal upwelling on the larval stage of the sardine.

Contrasting ecosystem responses to the weakening of coastal upwelling were observed in the outer and the inner shelf. In the outer shelf, the expected decrease of Chlorophyll *a* was confirmed by remote sensing observations but in the Rías chlorophyll shows a clear positive trend. This is due to the increase of dinoflagellates and *Pseudonitschia spp*. In addition, with a weaker upwelling, the flushing time in the inner shelf increased, consequently favoring stratification and an increase of the mineralization of organic matter which, in turn, lead to the observed positive trends of nitrite, ammonium and phosphate concentrations. These results indicate that the decline of coastal upwelling during the last three decades is driving the Iberian coastal ecosystem towards a less renewable condition, with more recycling and stratification. These changes in the ambient conditions are linked to two consequences of socioeconomic importance, namely, phytoplankton community successions that increase the frequency of HABs and the decline of sardine fisheries. A decreasing upwelling and decreasing rates for water renovation in the Rías lead to a lower productivity of exploitable species.

Acknowledgements

Authors thank Desmond Barton and two anonymous reviewers for comments that contributed to improvement of the manuscript. This study was partially funded by the European Commission (EU FP6 CARBOOCEAN Integrated Project, Contract no. 511176) and Xunta de Galiza (PGIDIT05PXIC40203PM, PGIDIT08MMA014402PR, PGIDIT07PXIB402153PR and PGIDIT05MA40201PR).

REFERENCES

Álvarez-Salgado XA *et al.* (2002) New Production of the NW Iberian Shelf during the Upwelling Season over the period 1982–1999. *Deep-Sea Res*. **49**:1725-1730.

Alvarez-Salgado XA, Castro CG, Pérez FF, Fraga F (1997) Nutrient mineralization patterns in shelf waters of the NW Iberian upwelling system. *Continental Shelf Research* **17**:1247–1270.

Alvarez-Salgado XA, Labarta E, Fernández-Reiriz XA *et al.* (2008) Renewal time and the impact of harmful algal blooms on the extensive mussel raft culture of the Iberian coastal upwelling system (SW Europe). *Harmful Algae* **7**, 849–855

Anderson DM (1997) Turning back the harmful red tide. *Nature* **388**:513-514.

Arístegui J, Alvarez-Salgado XA, Barton ED *et al.* (2004) Oceanography and Fisheries of the Canary Current/Iberian Region of the North Atlantic. In: *The Global Coastal Ocean: Interdisciplinary Regional Studies and Syntheses (The Sea: Ideas and Observations on Progress in the Study of the Seas, Vol. 14,* Eds. A.R. Robinson & K. Brink) chapter 23:877-931. Harvard University Press, Boston.

Bakun A (1973) Coastal upwelling indices, west coast of North America 1946–1971 *NOAA technical report, NMFSSSRF-* 671, 103 pp.

Bakun A (1990) Global climate change and intensification of coastal upwelling. *Science* **247**:198–201.

Bakun A, Weeks SJ (2004) Greenhouse gas buildup, sardines, submarine eruptions and the possibility of abrupt degradation of intense marine upwelling ecosystems. *Ecology Letters* **7**:1015–10232.

Barth JA *et al.* (2007) Delayed upwelling alters nearshore coastal ocean ecosystem in the northern California current. *Proceedings of the Natural Academy Science USA* **104**:3719-3724.

Behrenfeld MJ *et al.* (2006) Climate-driven trends in contemporary ocean productivity. *Nature* **444**:752-755.

Belgrano, A, Lindahl O, Hernroth B. (1999). North Atlantic Oscillation primary productivity and toxic phytoplankton in the Gullmar Fjord, Sweden (1985-1996).*Proceedings of the Royal Society of London - Series B: Biological Sciences* **266**:425-10.

Cabanas JM, Alvarez I (2005) Ekman transport patterns in the area close to the Galician coast (NW, Spain) *Journal. of Atmospheric and Ocean Scoence*, **10**, 325–341.

Carrera P, Porteiro C (2003) Stock dynamics of the Iberian sardine (Sardina pilchardus, W.) and its implication on the fishery off Galicia (NW Spain). *Scientia Marina* **67**(Suppl. 1):245-258.

Di Lorenzo E, Miller AJ, Schneider N, McWilliams JC (2005) The Warming of the California Current System: Dynamics and ecosystem implications. *Journal of Physical Oceanography,* **35**(3): 336–362 DOI: 10.1175/JPO-2690.1

Dickson RR, Nelly PM, Colebrook JM, Wooster WS, Cushing DH (1988) North winds and production in the eastern North Atlantic. *Journal of Plankton Research* **10**, 151-169.

Eppley RW, BJ Peterson (1979) Particulate organic matter flux and planktonic new production in the deep ocean. *Nature* **282**, 677-680.

Folland, CK, Knight, J, Linderholm H *et al.* (2009). The summer North Atlantic Oscillation: past, present and future. *Journal of Climate*. DOI: 10.1175/2008JCLI2459.1 (in press)

Fraga F (1981) in *Coastal Upwelling Series*, ed Richards FA (AGU), pp 176–182. Washington, DC

Global Ecology and Oceanography of Harmful Algal Blooms, 2005. In: Pitcher G, Moita T, Trainer, V, Kudela R, Figueiras, FG, Probyn T (Eds.), GEOHAB Core Research Project: HABs in Upwelling Systems. IOC and SCOR, Paris and Baltimore, p. 82.

Gregg WW, Casey NW, McClain CR (2005) Recent trends in global ocean chlorophyll. *Geophysical Research Letters* **32**:L03606.

Hansen HP, Grasshoff K (1983) Automated chemical analysis. In: Grasshoff, K, Ehrhardt, M, Kremling, K. (Eds.), In: *Methods of Seawater Analysis*. Verlag Chemie, Weinheim, pp. 347–395.

ICES, (2007) Report of the ICES Advisory Committee on Fisheries Management, Advisory Committee on the Marine Environment and Advisory Committee on Ecosystems. ICES Advice. Book **7**, 49-56.

Irigoyen X, Harris RP, Head RN, Harbour D (2000) North Atlantic Oscillation and spring bloom phytoplankton composition in the English Channel. *Journal of Plankton Research* **22** 2367-2371.

Johns DG, Edwards M, Richardson A, Spicer JI (2003) Increased blooms of a dinoflagellate in the northwest Atlantic. *Marine Ecology Progress Series* **265**:283-287.

Jossi JW, John AWG, Sameoto D (2003) Continuous Plankton Recorder sampling off the east coast of North America: history and status. *Progress in Oceanography* **58***:* 313–325

Kalnay E *et al.* (1996) The NCEP/NCAR 40-year reanalysis project, *Bulletin American Meteorological Society* **77**:437-470.

Longhurst A, (1996) Ecological Geography of the sea. Academic Press, San Diego, CA, 398 pp.

Margalef R, Estrada M, Blasco D (1979) in Toxic Dinoflagellate Blooms, eds Taylor D, Seliger H pp 89–94. Elsevier, New York.

Marshall J, Kushnir Y, Battisti D *et al.* (2001) North Atlantic Climate Variability: Phenomena, Impacts and Mechanisms. *International Journal of Climatology* **21**: 1863–1898.

McGregor HV, Dima M, Fischer HW, Mulitza S (2007) Rapid 20th–Century Increase in Coastal Upwelling off Northwest Africa. *Science* **315**:637–639.

Pauly D, Christensen V (1995) Primary production required to sustain global fisheries. *Nature* **374**:255-257.

Pazos Y, Figueiras FG, Álvarez-Salgado XA, Rosón G (1995) in *Harmful Marine Algae Blooms*, eds Lassus P, Arzul G, Erard E, Gentien P, Marcaillou C (Lavoisier, Intercept Ltd), pp 645-650.

Pazos Y, Maneiro J (1994) Algal bloom detection, monitoring and prediction in the Galician Rias (NW Spain), in '*Algal bloom detection, monitoring and prediction. 3th Workshop: Public Health*', G. Catena and E. Funari, Eds (Istituto Superiore di Sanita, Roma). pp 78-98.

Pérez FF, Álvarez–Salgado XA, Rosón G (2000) Stoichiometry of nutrients (C, N, P and Si) consumption and organic matter production in a coastal inlet affected by upwelling. *Marine Chemistry* **69**:217–236.

Pingree RD, Le Cann B, (1990) Structure, strength and seasonality of the slope currents in the bay of Biscay region. *Journal Marine Biological Association U.K*, **70**, 857–885.

Rosón G, Alvarez-Salgado XA, Pérez FF (1997) A Non-stationary Box Model to Determine Residual Fluxes in a Partially Mixed Estuary, Based on Both Thermohaline Properties: Application to the Ría de Arousa (NW Spain). *Estuarine Coastal and Shelf Science* **44**:249–262.

Sellner KG, Doucette GJ, Kirkpatrick GJ (2003) Harmful Algal Blooms: Causes, impacts, and detection. *Journal of Industrial Microbiology and Biotechnology* **30**:383-406.

Smayda TJ, Borkman D, Beaugrand G, Belgrano A (2004) in *Marine Ecosystems and Climate Variation* -- the North Atlantic, eds Stenseth NC, Ottersen G, Hurrell JW, Belgrano A, Planque B. Oxford University Press, Oxford, pp 49-58.

Smayda TJ, Reynolds CS (2001) Community assembly in marine phytoplankton: Application of recent models to harmful dinoflagellate blooms. *Journal of Plankton Research* **23**:447-461.

Sutherland TS et al, (1987) A segmented pipe sampler for integrated profiling of upper water column. *Journal of Plankton Research* **14**:915-923.

Tomczak M, Godfrey JS (2003) Regional Oceanography: An Introduction (Daya, Delhi, 2nd ed.)

Visbeck MH, Hurrell JW, Polvani L, Cullen HM 2001. The North Atlantic Oscillation: past, present, and future. *Proceedings of the Natural Academy Science USA* **98** doi:10.1073/pnas.231391598.

Wasmund N, S Uhlig (2003),Phytoplankton trends in the Baltic Sea. ICES Journal of Marine Science, **60**: 177–186. 2003. doi:10.1016/S1054–3139(02)00280-1.

Wiltshire KH, Manly BFJ (2004) The warming trend at Helgoland Roads, North Sea: phytoplankton response. *Helgoland Marine Research* (2004) **58**: 269–273. DOI 10.1007/s10152-004-0196-0.

Wooster WS, Bakun A, McLain DR (1976) The seasonal upwelling cycle along the eastern boundary of the North Atlantic. *Journal of Marine Research* **34**:131-140.

Zapata M, Maneiro J, Muñiz S, Blanco J, Mariño J (1994), in '*Tercera Reunión Ibérica sobre fitoplancton tóxico y biotoxinas*', J. Mariño and J. Maneiro Eds (Xunta de Galicia). Santiago Compostela pp 47.

Correspondence and requests for materials should be addressed to F.F.P. (fiz.perez@iim.csic.es).

Acronyms:
BV: Brunt-Väisälä frequency
HAB: Harmful Algal Bloom;
ICES: International Council for the Exploration of the Sea; Chl a: Chlorophyll a;
NEP: Net Ecosystem Production.
NP: New Production;
SLP: Sea Level Pressure;
MODIS: Moderate Resolution Imaging Spectroradiometer
NCEP: National Centers for Environmental Prediction;
SST: Sea Surface Temperature;
SeaWIFS: Sea-viewing Wide Field-of-view Sensor

LEGEND OF FIGURES

FIGURE 1: The color contour map shows the sea surface temperature (SST) increment of summer averages (June-August) between 1973-1975 and 2001-2003 calculated with the monthly means of NCEP Reanalysis provided by the NOAA/OAR/ESRL PSD, Boulder, Colorado, USA (http://www.cdc.noaa.gov/). Superimposed are the average sea level pressure (SLP) contour lines (in hPa) for the same summer periods (red line: 1973-1975 and black line: 2001-2003), also taken from the NCEP dataset. The pink line along 43ºN highlights the change in the gradient of SLP in the vicinity of Galician coast between the two periods analyzed. The inset map encloses the coastal area under the influence of upwelling events. The chlorophyll *a* dataset of Fig. 4 was taken in the outer shelf dotted area. The annual evolution and long-term trend of upwelling index are plotted in Fig. 2 for two locations: 43ºN 11ºW (green dot) and 42.85ºN 9.37ºW (red dot). The orange dot indicates the mouth of the Ría de Arousa, where the dataset of Fig. 4 was sampled. The purple circle denotes Cape Ghir.

FIGURE 2: Annual evolution and long-term trends of two different upwelling indices (Iw) from 1965 to 2007: SLP Iw (black line and grey circles, using geostrophic winds at 43ºN 11ºW, green dot in Fig. 1), NCEP Iw (red line and white circles, using reanalysis winds at 42.85ºN 9.37ºW, red dot in Fig. 1). The linear interannual trend of SLP Iw and NCEP Iw are shown as black and pink lines, respectively. The orange bars depict the time series of sea surface temperature annual anomaly (ΔSST) with respect to the 1965 – 2007 mean value (14.87ºC) at the red dot in Fig. 1. The grey crosshatch areas correspond to the two periods analyzed in Fig. 1 (1973-1975 and 2001-2003).

FIGURE 3: Net Production (light pink circles) and its 3-year moving average (grey line) in the outer shelf of Galician coast. Iberian sardine (*Sardine pilchardus*) landings (light blue circles), and its 3-year moving average (dark blue line) for the period 1965 to 2006 in ICES Division VIIIc.

FIGURE 4: Time series of monthly averaged hydrographic and phytoplankton variables recorded in the mouth of Ría de Arousa from 1992 to 2007. a) Sea surface temperature (red circles). b) Chlorophyll *a* concentration (green circles) in the inner shelf and satellite derived Chlorophyll *a* (yellow symbols) in the open ocean water (dotted area and orange circle in inlet of Fig. 1, respectively). c) Diatomea abundances (light blue circles). d) Logarithm of percentage of dinoflagellates with respect to total phytoplankton (orange circle). e) *Pseudonitzschia spp* abundances (solid pink circles). f) Nitrite (NO_2) concentration (white circle). g) Phosphate (PO_4) concentration (grey circle). The yellow dots and squares in panel b stand for the SeaWiFS and MODIS chlorophyll *a*, spatially averaged in the dotted area of Fig. 1 inset (standard deviation as error bars).

Figure 1

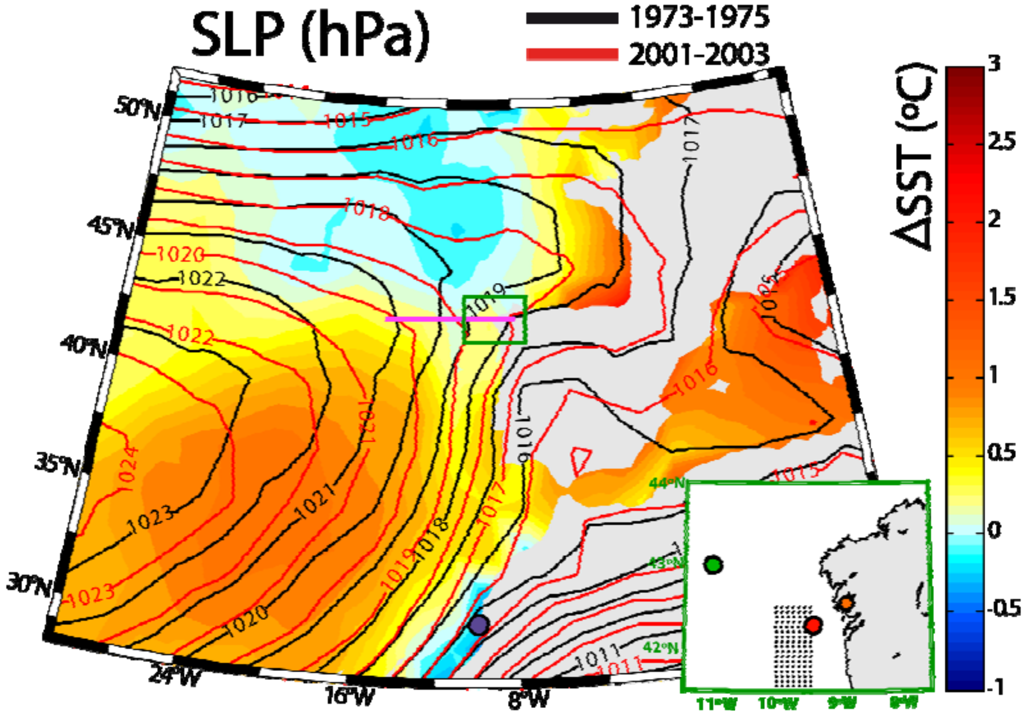

Figure 2

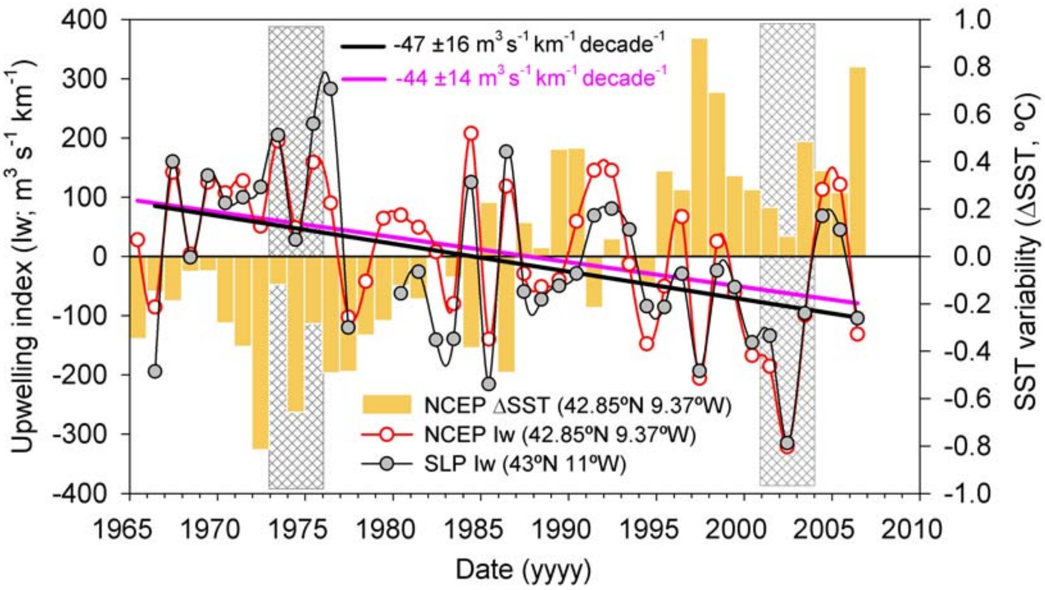

Figure 3

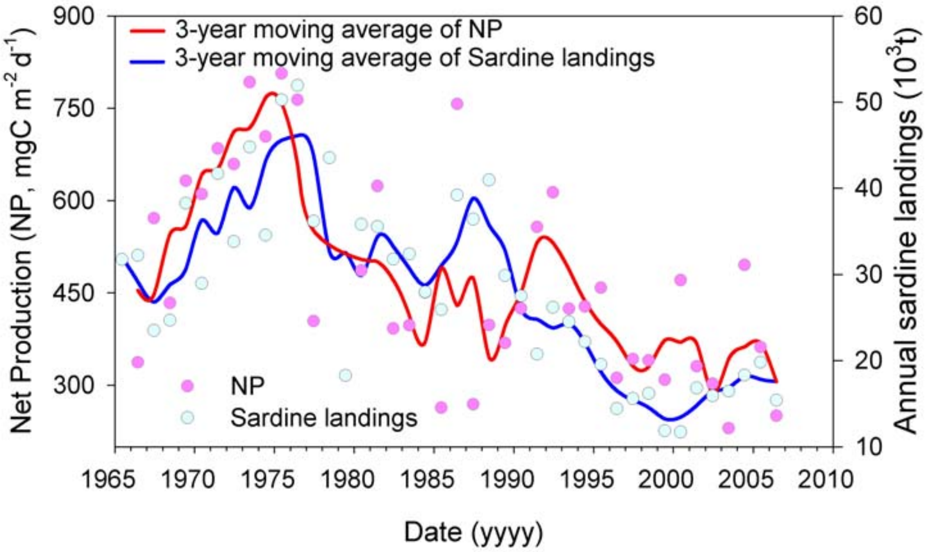
3-year moving average of NP
3-year moving average of Sardine landings
NP
Sardine landings
Net Production (NP, mgC m-2 d-1)
Annual sardine landings (10^3 t)
Date (yyyy)
900
750
600
450
300
60
50
40
30
20
10
1965
1970
1975
1980
1985
1990
1995
2000
2005
2010

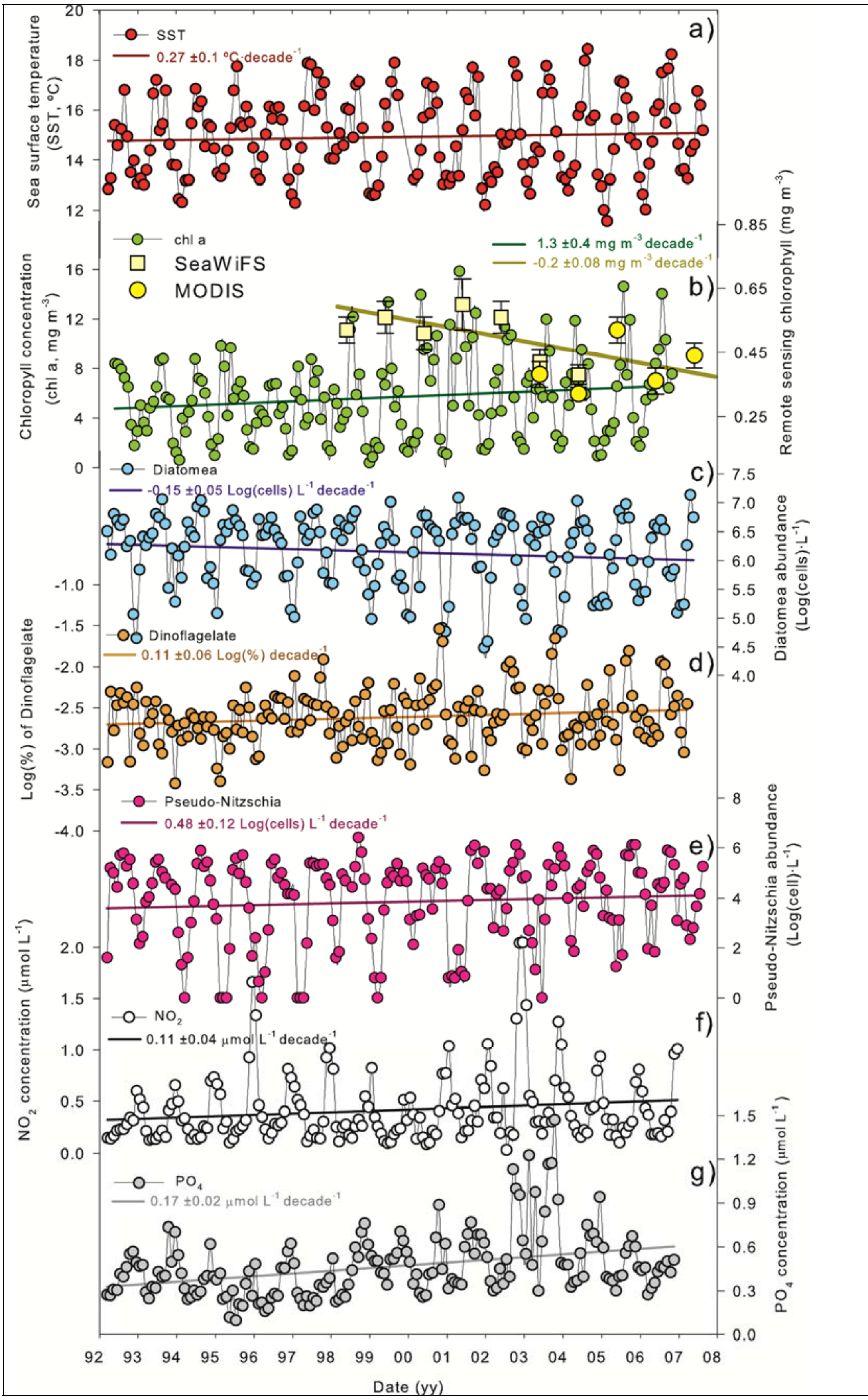
SST
0.27 ±0.1 °C decade-1
a)
Sea surface temperature (SST, °C)
chl a
SeaWiFS
MODIS
1.3 ±0.4 mg m-3 decade-1
-0.2 ±0.08 mg m-3 decade-1
b)
Chlorophyll concentration (chl a, mg m-3)
Remote sensing chlorophyll (mg m-3)
Diatomea
-0.15 ±0.05 Log(cells) L-1 decade-1
c)
Diatomea abundance (Log(cells)·L-1)
Dinoflagelate
0.11 ±0.06 Log(%) decade-1
d)
Log(%) of Dinoflagelate
Pseudo-Nitzschia
0.48 ±0.12 Log(cells) L-1 decade-1
e)
Pseudo-Nitzschia abundance (Log(cell)·L-1)
NO2
0.11 ±0.04 µmol L-1 decade-1
f)
NO2 concentration (µmol L-1)
PO4
0.17 ±0.02 µmol L-1 decade-1
g)
PO4 concentration (µmol L-1)
Date (yy)

Figure 4

1

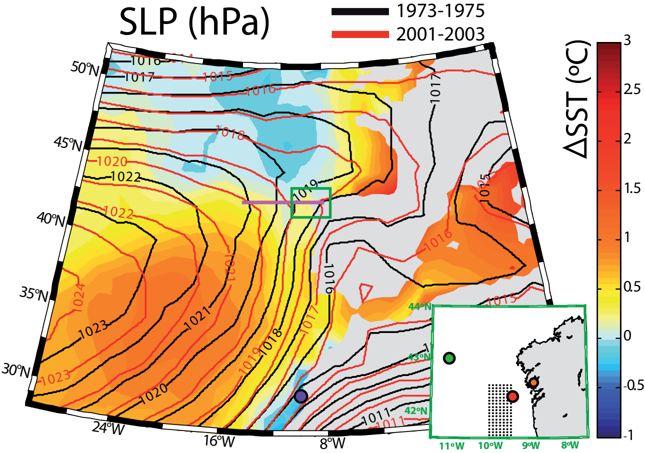

SLP (hPa)
1973-1975
2001-2003
ΔSST (ºC)
3
2.5
2
1.5
1
0.5
0
-0.5
-1
50ºN
45ºN
40ºN
35ºN
30ºN
24ºW
16ºW
8ºW
1016
1017
1015
1018
1019
1020
1021
1022
1023
1024
1011
44ºN
43ºN
42ºN
11ºW
10ºW
9ºW
8ºW

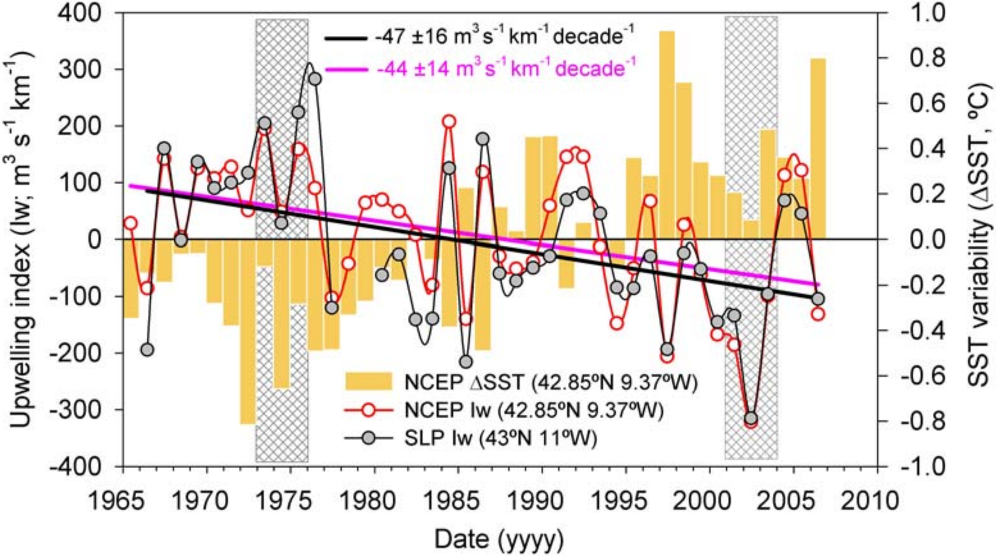
-47 ±16 m3 s-1 km-1 decade-1
-44 ±14 m3 s-1 km-1 decade-1
NCEP ΔSST (42.85ºN 9.37ºW)
NCEP Iw (42.85ºN 9.37ºW)
SLP Iw (43ºN 11ºW)
Upwelling index (Iw; m3 s-1 km-1)
SST variability (ΔSST, ºC)
Date (yyyy)
400
300
200
100
0
-100
-200
-300
-400
1.0
0.8
0.6
0.4
0.2
0.0
-0.2
-0.4
-0.6
-0.8
-1.0
1965
1970
1975
1980
1985
1990
1995
2000
2005
2010

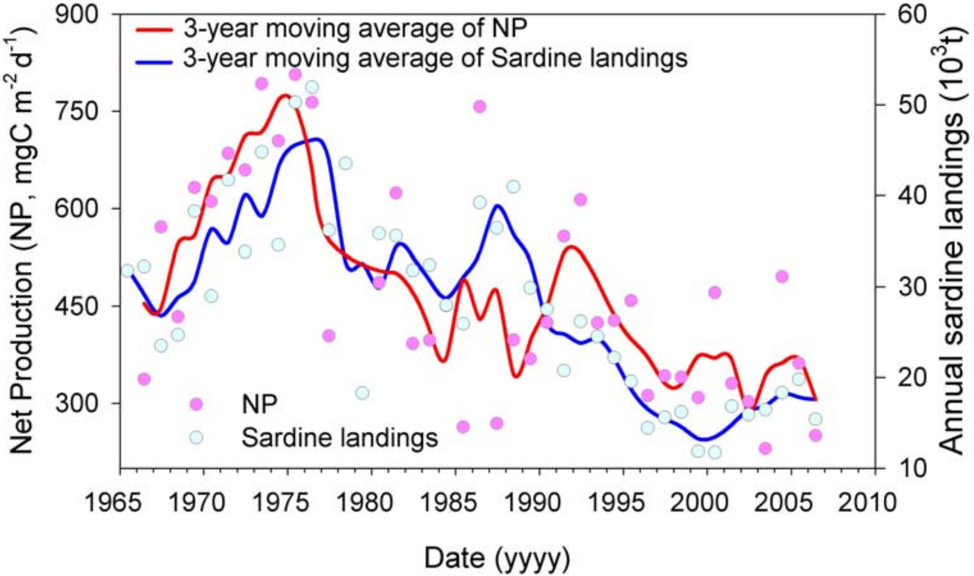

3-year moving average of NP
3-year moving average of Sardine landings
NP
Sardine landings
Net Production (NP, mgC m-2 d-1)
Annual sardine landings (10^3 t)
Date (yyyy)
900
750
600
450
300
60
50
40
30
20
10
1965
1970
1975
1980
1985
1990
1995
2000
2005
2010

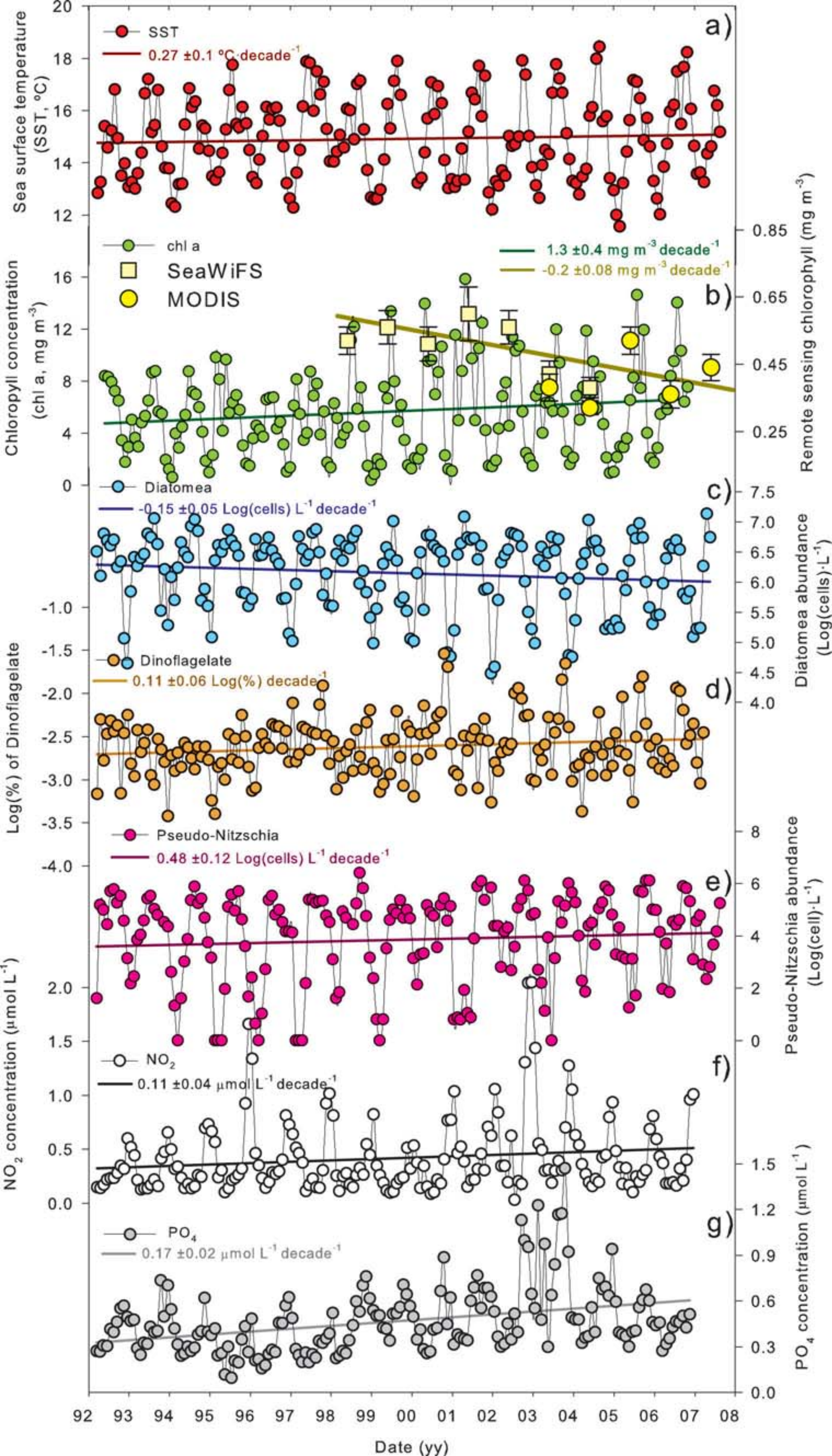

SST
0.27 ±0.1 °C·decade⁻¹
a)
Sea surface temperature (SST, °C)
chl a
SeaWiFS
MODIS
1.3 ±0.4 mg m⁻³ decade⁻¹
-0.2 ±0.08 mg m⁻³ decade⁻¹
b)
Chloropyll concentration (chl a, mg m⁻³)
Remote sensing chlorophyll (mg m⁻³)
Diatomea
-0.15 ±0.05 Log(cells) L⁻¹ decade⁻¹
c)
Diatomea abundance (Log(cells)·L⁻¹)
Dinoflagelate
0.11 ±0.06 Log(%) decade⁻¹
d)
Log(%) of Dinoflagelate
Pseudo-Nitzschia
0.48 ±0.12 Log(cells) L⁻¹ decade⁻¹
e)
Pseudo-Nitzschia abundance (Log(cell)·L⁻¹)
NO2
0.11 ±0.04 μmol L⁻¹ decade⁻¹
f)
NO2 concentration (μmol L⁻¹)
PO4
0.17 ±0.02 μmol L⁻¹ decade⁻¹
g)
PO4 concentration (μmol L⁻¹)
Date (yy)